行政院國家科學委員會專題研究計畫 成果報告

鎂合金高溫變形機制及快速塑性成形(QPF)研究
研究成果報告(精簡版)

計 畫 類 別 ：個別型
計 畫 編 號 ：NSC 99-2221-E-216-005-
執 行 期 間 ：99 年 08 月 01 日至 100 年 07 月 31 日
執 行 單 位 ：中華大學機械工程學系

計 畫 主 持 人：吳泓瑜

計畫參與人員：碩士班研究生-兼任助理人員：廖經皓
碩士班研究生-兼任助理人員：林政宇
大專生-兼任助理人員：朱峰君
博士班研究生-兼任助理人員：孫稟厚

處 理 方 式 ：本計畫可公開查詢

中 華 民 國 100 年 09 月 20 日

行政院國家科學委員會專題研究計畫成果報告

鎂合金高溫變行機制及快速塑性成形(QPF)研究

High temperature deformation mechanisms and quick plastic forming (QPF) in Mg alloy

計畫編號：NSC 99-2221-E-216-005

執行期間：99年 8月 1日至100年 7月31日

計畫主持人: 吳泓瑜　　中華大學機械工程學系教授

E-mail: ncuwu@chu.edu.tw

計畫參與人員：廖經皓、林政宇、朱峰君 中華大學機械工程學系研究生

中文摘要

本研究主要目的是減少細晶結構AZ31B鎂合金板材的氣壓成形時間，板材厚度為0.6毫米；並以拉伸試驗和氣壓成形來探討薄板的變形行為。由拉伸實驗應力–應變速率資料的關係圖顯示，細晶AZ31B鎂合金板材在測試溫度為350 °C，應變速率範圍為4×10^{-3} 至 2×10^{-2} s^{-1}的變形條件下，應變速率敏感指數值約為0.26。這項結果顯示，差排潛變是一個可能的變形機制用來減少氣壓成形所需要的成形時間。使用快速氣壓成形的加壓程序，成功地將合金板材製作成淺長方形的和狀試件。對於快速氣壓成形的特性進行了討論。研究結果顯示，使用傳統母模的成形方式，以差排潛變產生的變形條件進行氣壓成形，成形時間可以顯著地減少。在本研究中，淺長方形盒狀試件的深度約為10毫米，在350 °C的成形溫度下，所需成形時間可以少於165秒。成形溫度、加壓程序的影響、及成形試件的變形特性也進行了分析。就盒狀試件而言，圓角半徑的大小是影響成形時間的關鍵因素之一。

關鍵詞：差排潛變、R角半徑、細晶AZ31B鎂合金、快速氣壓成形、應力指數

Abstract

This work studied the decrease in forming time in gas blow forming in the fine-grained AZ31B Mg alloy sheet with a thickness of 0.6 mm. Tensile tests and gas blow forming were performed to explore the deformation behavior. The stress-strain rate data showed that the fine-grained AZ31B Mg alloy sheet on testing at 350 °C exhibited strain rate sensitivity exponent value of approximately 0.26 in a strain rate ranging from 4×10^{-3} and 2×10^{-2} s^{-1}, indicating that the dislocation creep would be a possible deformation mechanism to reduce forming time in gas blow forming. The alloy sheets were successfully deformed into shallow rectangular pans using rapid gas pressure forming. The deformation characteristics of gas blow forming were discussed. As a result, a significant reduction in forming time was achieved using traditional female

die forming, in which a rectangular pan was formed with a height of 10 mm in less than 165 s at 350 °C. Fillet radius of the rectangular pan should be one of the key factors influencing forming time.

Keywords: Dislocation creep; Fillet radius; Fine-grained AZ31B Mg alloy; Rapid gas blow forming; Stress exponent.

1. Introduction

Recently, the desire to reduce vehicle weight and improve fuel efficiency has raised the need for the deformation of large complex-shaped products made of Mg alloys. Carpenter et al. [1] reported that research and development in North America on magnesium for automotive applications and also indicated that Mg alloy is a promising candidate for light weighting. Conventional stamping of Mg alloys into sheet parts is limited by their relatively low formability. Superplastic forming (SPF) is an effective method to overcome this limitation. From the viewpoint of applied mechanics, one of the most important characteristics of superplastic materials is their high strain-rate sensitivity of flow stress. The strain-rate sensitivity exponent, m (in the approximation of $\sigma = K\dot{\varepsilon}^m$), is the key in controlling the ductility of a superplastic material at elevated temperatures. In other words, the higher the value of m, the higher is the necking resistance. However, fine-grained superplastic materials exhibit high m-values only in a narrow range of strain rates, thus requiring careful process control to maintain the desired constant strain rate during SPF. Yin et al. [2] showed that a superplastic elongation of 362.5% is obtained in AZ31 Mg alloy at the temperature of 400 °C and strain rate of 7×10^{-4} s^{-1}. Abu-Farha and Khraisheh [3] reported that approximately 10^{-3} s^{-1} strain rate is the threshold for superplasticity in AZ31alloy. A significant problem in the commercial application of SPF on AZ31B alloy is the low deformation rates (10^{-3}–10^{-4} s^{-1}), which is undesirable in mass production.

Superplasticity corresponds to deformation conditions in which grain boundary sliding (GBS) is the dominant controlling mechanism, with an m-value of close to 0.5. However, the dislocation creep is expected to be the major deformation mechanism at higher strain rates and/or at lower temperatures. Non-superplastic behavior in AZ31 alloy with an m-value of 0.2 has been reported by Panicker et al. [4]. Watanabe et al. [5] showed that at strain rates over 1×10^{-2} s^{-1} at 548 K, m decreased to a small value, indicating that deformation probably corresponds to dislocation creep. Although the m-value of dislocation creep is not as high as that of GBS creep, dislocation creep produces medium strain-rate sensitivity exponent (m = 0.33 to 0.2) and can provide sufficient tensile ductility. Watanabe et al. [6] reported that a high ductility of 196% at 375 °C observed in a coarse-grained AZ31 Mg alloy is attributed to the deformation mechanism of glide-controlled dislocation creep. Del Valle et al. [7] indicated that the enhanced ductility of the AZ31 alloy in the lower strain-rate regime is attributed to the concurrent operation of GBS and crystallographic slip. These results indicate

that the dislocation creep can be the controlling mechanism for a fine-grained AZ31B Mg alloy, and that the gas blow forming process with a higher pressurization rate can be used to reduce forming time. Chung et al. [8] demonstrated constant gas pressure forming of a fine-grained AZ61 magnesium alloy sheet. A hemispherical cap was successfully produced using a forming time of 250 s at 375 °C with an applied pressure of 1.20 MPa, in which the maximum average strain rate of 4.77×10^{-3} s^{-1} was attained at the apex of the formed cap. Kim et al. [9] also demonstrated the superplastic formability of an AZ31 alloy sheet using a two-step pressurization profile. A 250 × 250 mm panel with complicated embossing patterns can be completely formed at 400 °C with a forming time of 800 s.

In the present study, the deformation characteristics of a commercial-grade fine-grained AZ31B alloy sheet using uniaxial tension and gas blow forming were investigated. Shallow rectangular pans were gas blow formed demonstrating the possibility of rapid gas blow forming for industrial applications. A detailed description on the deformation behavior of the fine-grained AZ31B Mg alloy sheet under conditions of uniaxial and biaxial tensile deformation was provided and deformation characteristics during gas blow forming were quantitatively analyzed.

2. Materials and experimental procedure

This work used the fine-grained AZ31B Mg alloy sheet with a thickness of 0.6 mm provided by Magnesium Elektron North American Inc., USA. The analyzed chemical composition was (wt-%) Mg-3.01Al-1.03Zn-0.22Mn and the average grain size was approximately 7.5 μm before forming. The optical image of the original sheet microstructure is presented in Fig. 1.

The sheet type tensile specimens were machined according to the ASTM B-557M standard procedure with a gauge length and width of 25 and 6 mm, respectively. Uniaxial tension tests were conducted along the rolling direction on the three samples for each test at temperatures from 250 to 400 °C and at constant crosshead speeds, giving initial strain rates in the range of 4×10^{-3} to 1×10^{-1} s^{-1}.

Traditional female die gas blow forming processes were carried out at a temperature of 350 °C. Shallow pans were formed by deforming the sheet into a rectangular die cavity. The die had a rectangular cavity of 110 mm (length) × 50 mm (width) × 10 mm (depth) with a die entry radius of 2 mm and a draft angle of 3°. Several interrupted tests were performed to deform the sheets to various degrees of heights for each test. Gas blow forming tests were conducted according to the pressure-time profiles shown in Fig. 2.

Grid circles of diameter d_0 (2.5mm) etched on the sheets were employed to measure the strain levels in each test. During forming the etched circles were distorted into ellipses. After deformation, measurements of the major and minor diameters, d_1 and d_2, respectively, were made to calculate the principal strains, effective strains, and average strain rates.

3. Results and discussion

3.1. Tensile tests

3.1.1 Tensile flow behavior

The uniaxial tensile curves obtained at a strain rate of 4×10^{-3} s^{-1} and various temperatures are given Fig. 3. The flow curve exhibits the power law constitutive relation until peak stress is reached. At this level, a softening region leading to fracture was observed. Additionally, a lower hardening effect and a longer softening region leading to fracture were noted on testing at higher temperatures. Fig. 4 shows the true stress–strain relationships of the fine-grained AZ31B Mg alloy sheet on testing at 400 °C and various strain rates. The flow curve in a relatively high strain rate range of 1×10^{-2} to 1×10^{-1} s^{-1} reaches a peak value, then decreases followed by fracture. The flow curve at a lower strain rate of 4×10^{-3} s^{-1} transforms into a steady-state regime, wherein the flow stress is almost independent of strain at higher strains.

The elongation to failure as a function of strain rate is given in Fig. 5. From the figure, tensile elongation evidently depends on the strain rate and temperature. The elongation to failure decreases with increasing strain rate, however, the extent of decrease depends on temperature. The effect of the strain rate on elongation is more pronounced at higher temperatures of 350–400 °C. A large elongation of more than 200% was attained in the strain rate range of under 10^{-2} s^{-1} at 400 °C.

3.1.2. Hot deformation characteristics

Jonas et al. [10] indicated that the constitutive equation to describe the high temperature deformation is generally expressed as

$$\dot{\varepsilon} = A\sigma^n \exp\left[\frac{-Q}{RT}\right] \quad (1)$$

where $\dot{\varepsilon}$ is the strain rate, A is a constant, σ is the flow stress, n is the stress exponent (=1/m, m is the strain rate sensitivity exponent), R is the gas constant, T is the absolute temperature and Q is the activation energy for diffusion, which is dependent on the rate controlling process. Eq. (1) can be rewritten as

$$\ln\sigma = \frac{1}{n}\ln\dot{\varepsilon} + \frac{Q}{nR}\left(\frac{1}{T}\right) - \frac{1}{n}\ln A \quad (2)$$

According to Eq. (2), n is the slope of the line in the plot of $\ln\dot{\varepsilon}$ versus $\ln\sigma$ at constant strain and temperature. The value of Q can be calculated using the slope of the line in the plot of $\ln\sigma$ versus $1/T$ at constant strain and strain rate.

With regard to the approximation, the peak stress is used as one of the representative flow stresses to evaluate the deformation mechanisms. The stress exponent, n, obtained in the present work was approximately 3.7–7.3 (m = 0.27–0.14), as shown in Fig. 6. The n-value can influence the deformation mechanism of the fine-grained alloys. Watanabe et al. [11] investigated the dominant diffusion process for superplastic flow in an AZ61 magnesium alloy. Their results indicated that the n-value of 2 suggests that GBS could be a dominant deformation process. For higher strain rates, the n-value is significantly increased to approximately 5, and the deformation mechanism is related to dislocation creep. Dislocation creep behavior in Mg–Al–Zn

alloys has been explored by Somekawa and coworkers [12]. Kulas and Green [13] reported that the *n*-value of approximately 3 is always found when dislocation creep is controlled by viscous glide. As the dislocation creep plays an important role in the deformation conditions, while simultaneously preserving significant capacity of deformation, considerable reduction in forming times can be achieved in gas blow forming. The tensile test results in the present work showed that the *n*-values were approximately 4 at higher temperatures, and approximately 7 at a lower temperature of 250 °C, respectively. Therefore, the fine-grained AZ31B Mg alloy sheet with *n*-values of approximately 4 is possible to be deformed at a strain rate in the order of approximately 10^{-2} s^{-1} and temperatures of 350–400 °C with sufficient ductility in gas blow forming.

The value of activation energy *Q* calculated using the slopes of the plots in Figs. 6 and 7 was approximately 94 kJ/mol. Frost and Ashby [14] demonstrated that the activation energy was 92 kJ/mol for pipe diffusion of magnesium. It is suggested from the stress exponent and the activation energy that the dominant deformation mechanism in the fine-grained AZ31B Mg alloy sheet is dislocation creep, which is controlled by pipe diffusion, under the deformation conditions performed in the present work.

3.2. Gas blow forming

3.2.1. Deformation contour

Fig. 8 illustrates the formed shallow rectangular pan to show the status of the deformed grid circles. The effect of imposed pressure on the deformation contour and metal flow for forming at two different pressurization profiles is depicted in Fig. 9. Forming at CP350-165 with a lower imposed pressure of 2.6 MPa results in lower surface friction between the deformed sheet and bottom surface of the die after the sheet touches the die. Some displacement of metal flow could be observed for the overlaid region, as shown in Fig. 9(a). Metal flow moves from the bottom center and die entry region toward the bottom corner. A greater interfacial friction alters the metal flow for forming at CP350-106 with a higher imposed pressure of 3.2 MPa. Metal flow moves from the bottom center and die entry region toward the location near the bottom corner on the die bottom surface, as shown in Fig. 9(b). Fig. 9 also indicates that forming at CP350-165 with a lower imposed pressure exhibits greater displacement of the overlaid region compared to that of forming at CP350-106 with a higher imposed pressure. In a constant pressure forming with a die cavity having a half-width greater than its depth, the deformed sheet quickly comes in contact with the bottom surface of the die cavity (Fig. 9), however, it needs much more time for the sheet to make contact with the die walls.

3.2.2. Die fillet radius evolution

In order to quantify the die filling behavior, the fillet radius of the formed pan was measured. The fillet radius evolution can be used to analyze the die filling behavior. Variation in the fillet radius as a function of forming time is given in Fig. 10. A nonlinear relationship between fillet

radius and forming time was observed. Variations in fillet radius with forming time are similar for both pressurization profiles. The reduction in fillet radius can be characterized by three distinctive regions: initially, the radius decreases rapidly, then a lower reduction rate stage is reached, and finally, a quite low decreasing rate occurs in the later stage of forming. The final fillet radii are 1.7 and 1.5 mm for forming at CP350-105 and CP350-165, respectively. It takes approximately 90 and 60 s for the fillet radii reducing from 2.0 to 1.5 mm and from 2.5 to 1.7 mm for forming at CP350-165 and CP350-106, respectively. These results imply that the fillet radius is one of the key factors influencing forming time for closed die gas blow forming. Although a smaller fillet radius can be reached, the forming time may increase tremendously. The forming time for forming a component with a very small fillet radius appears non-cost effective for industrial applications.

3.2.3. Thickness evolution

Thickness evolution at the center point of the deformed sheet with forming time is given in Fig. 11. Different thinning behaviors were observed for forming at different pressurization profiles. At the beginning of forming, the thickness decreases rapidly with forming time for both pressurization profiles. Then, after the sheet comes in contact with the bottom surface of the die, the thickness still decreases with forming time for forming at CP350-165, whereas the thickness remains constant for forming at CP350-106. The thinning behavior can be associated with the pressure imposed during forming. After the sheet has been overlaid on the die surface, surface friction restricts the metal flow of the overlaid region. A higher pressure of 3.2 MPa imposed for forming at CP350-106 provides more restriction on the metal flow, resulting in a constant thickness at the center point in the later stage of forming. These results are consistent with the metal flow shown in Fig. 9.

3.2.4. Thickness distribution

The effect of imposed pressure on the thickness distribution of the formed rectangular pan is demonstrated in Fig. 12. Different distributions in thickness along the transverse cross-section were observed for forming at two different pressures. The thinnest positions locate at approximately 18 and 20 mm away from the bottom center of the formed pan for forming at CP350-106 and CP350-165, respectively. However, a more uniform thickness distribution was observed for forming at CP350-165. The degree of the interfacial friction influences the metal flows after contacting, and the interfacial friction is large for forming at CP350-106. When the sheet comes in contact with the die surface, the deformation in that contact area is restricted. Additionally, thinning is localized in the non-contact areas, resulting in a greater degree of thinning. If the interfacial friction is reduced, such as in the case where a lower pressure of 2.6 MPa is applied, the thinning gradient of the formed part is reduced because continued metal flow after contact is possible. The thinning effect of the deformed sheet on forming at CP350-165 continues to take

place in the overlaid region during forming, which also leads to the shift in the thinnest position slightly further away from the bottom center than that for forming at CP350-106.

3.2.5. Average strain rate distribution

The average strain rate distribution along the transverse cross-section of the formed rectangular pan for forming at two different pressures is shown in Fig. 13. The average strain rate for forming at CP350-106 is higher than that for forming at CP350-165 because of a higher pressure imposed for forming at CP350-106. The maximum average strain rates are 3.8×10^{-3} and 2.5×10^{-3} s^{-1} for forming at CP350-106 and CP350-165, respectively. Fig. 13 also shows that the location of the maximum average strain rate shifts downward to the position near the bottom corner for forming at CP350-106 because of the effect of higher interfacial friction restricting the metal flow of the overlaid region on the bottom surface of the die.

4. Conclusions

Deformation characteristics of the fine-grained AZ31B Mg alloy sheet were studied using tensile tests and constant pressure gas blow forming. Detailed uniaxial and biaxial experiments clearly indicated the effectiveness of constant pressure forming in reducing forming time. Tensile test results indicated that dislocation creep is the major rate-controlling mechanism at a strain rate in the order of 10^{-2} s^{-1} for the fine-grained AZ31B Mg alloy sheet, and reducing forming time is possible by gas blow forming.

A shallow rectangular pan with a width to depth ratio of 5 was also successfully formed in less than 165 s. Constant pressure forming of the fine-grained AZ31B Mg alloy sheet showed its potential for future practical applications. Variation in the fillet radius of the formed pan with forming time indicated that the forming time was strongly dependent on the fillet radius. Fillet radius of 1.5 mm was achieved for forming at a pressure of 2.6 MPa in 165 s. A smaller fillet radius might tremendously increase the forming time. A compromise between the designed fillet radius and the forming time might be necessary to meet the requirements of mass production.

References

[1] J.A. Carpenter, J. Jackman, N. Li, R.J. Osborne, B.R. Powell, P. Sklad, Mater. Sci. Forum 546-549 (2007) 11–24.

[2] D.L. Yin, K.F. Zhang, G.F. Wang, W.B. Han, Mater. Letters 59 (2005) 1714–1718.

[3] F.K. Abu-Farha, M.K. Khraisheh, J. Mater. Eng. Perform. 16 (2007) 192–199.

[4] R. Panicker, A.H. Chokshi, R.K. Mishra, R. Verma, P.E. Krajewski, Acta Mater. 57 (2009) 3683–3693.

[5] H. Watanabe, M. Fukusumi, H. Somekawa, T. Mukai, Mater. Sci. Eng. A 527 (2010) 6350–6358.

[6] H. Watanabe, H. Tsutsui, Y. Mukai, M. Kohzu, S. Tanabe, K. Higashi, Intern. J. Plast. 17 (2001) 387–397.

[7] J.A. Del Valle, M.T. Perez-Prado, O.A.

Ruano, Metall. Mater. Trans. A 36 (2005) 1427–1438.

[8] S.W. Chung, K. Higashi, W.J. Kim, Mater. Sci. Eng. A 372 (2004) 15–20.

[9] W.J. Kim, J.D. Park, U.S. Yoon, J. Alloys Compd. 464 (2008) 197–204.

[10] J.J. Jonas, C.M. Sellars, W.J. McG. Tegart, Metall. Rev. 14 (1969) 1–24.

[11] H. Watanabe, T. Mukai, M. Kohzu, S. Tanabe, K. Higashi, Acta Mater. 47 (1999) 3753–3758.

[12] H. Somekawa, K. Hirai, H. Watanabe, Y. Takigawa, K. Higashi, Mater. Sci. Eng. A 407 (2005) 53–61.

[13] M.A. Kulas, W.P. Green, E.M Taleff, P.E. Krajewski, T.R. McNelley, Metall. Mater. Trans. A 36 (2005) 1249–1261.

[14] H.J. Frost, M.F. Ashby, Deformation-Mechanism Maps, Pergamon Press, Oxford, (1982) pp. 43–44.

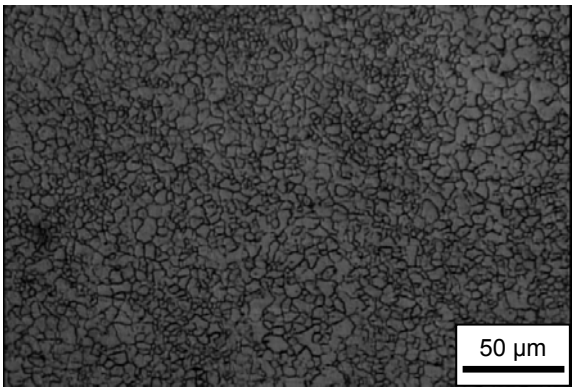

Fig. 1. Optical image of the microstructure of the fine-grained AZ31B Mg alloy sheet.

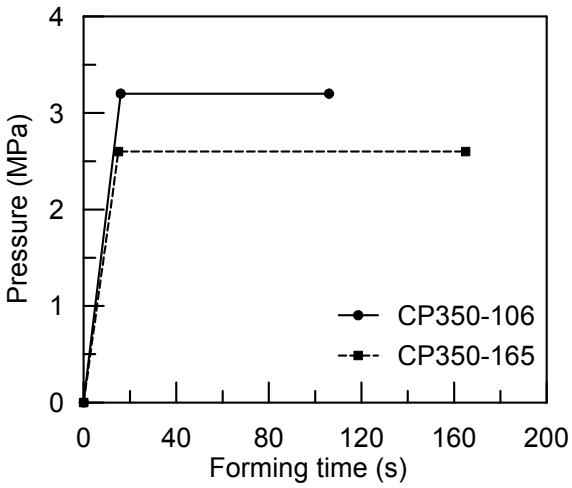

Fig. 2. Pressure–time profiles for hot rapid gas blow forming.

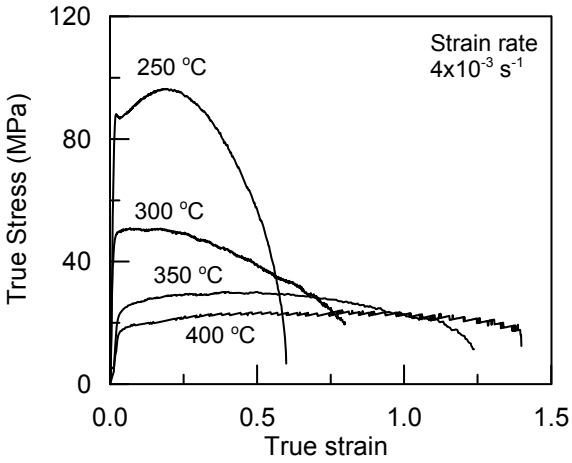

Fig. 3. Tensile flow curves of the specimens tested at a strain rate of 4×10^{-3} s^{-1} and various temperatures.

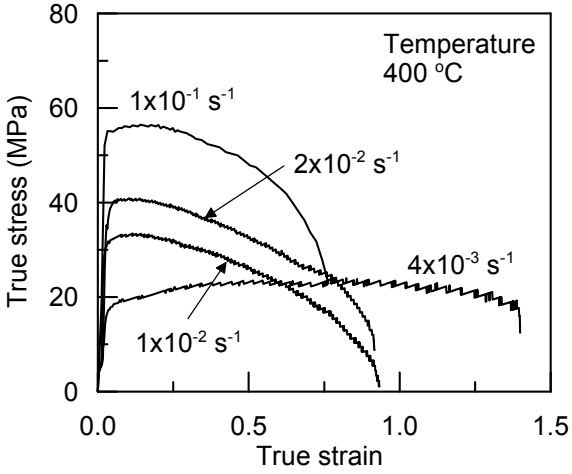

Fig. 4. Tensile flow curves of the specimens tested at 400 °C and various strain rates.

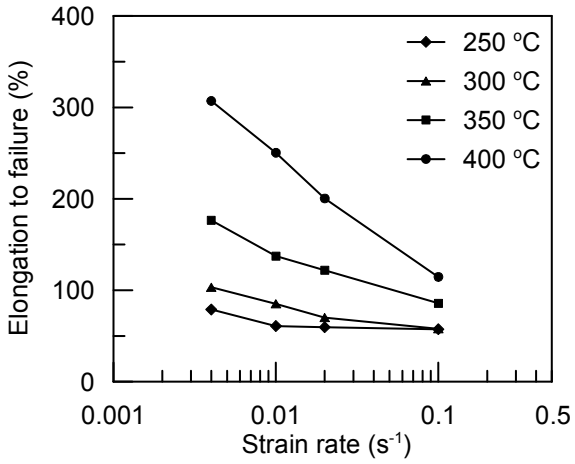

Fig. 5. Elongation to failure for the fine-grained AZ31B Mg alloy sheet plotted as a function of log initial strain rate for samples tested at various temperatures.

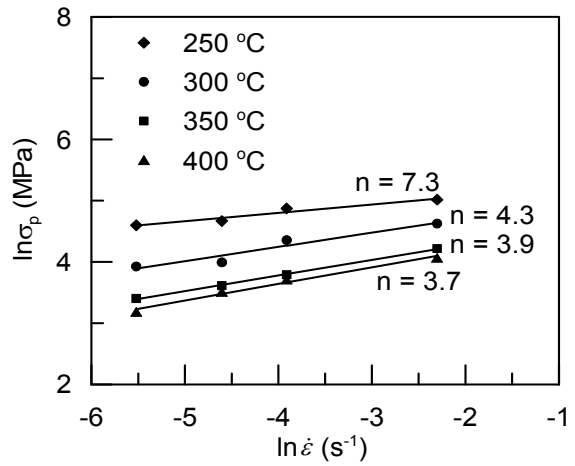

Fig. 6. Variation in peak stress as a function of strain rate.

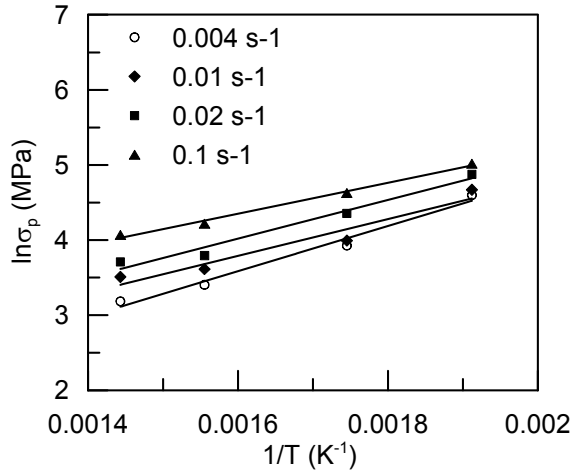

Fig. 7. Variation in peak stress as a function of reciprocal temperature.

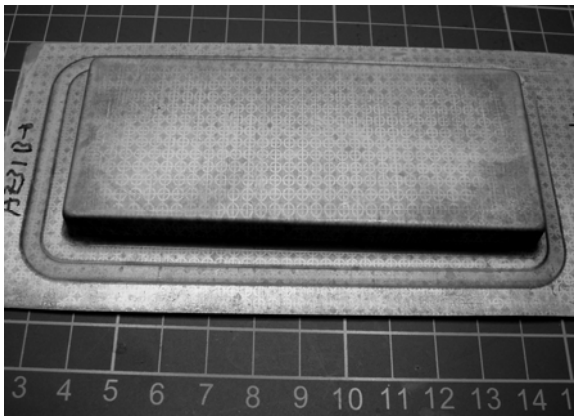

Fig. 8. Image of the formed shallow rectangular pan using traditional female die gas blow forming to demonstrate the deformed grid circles.

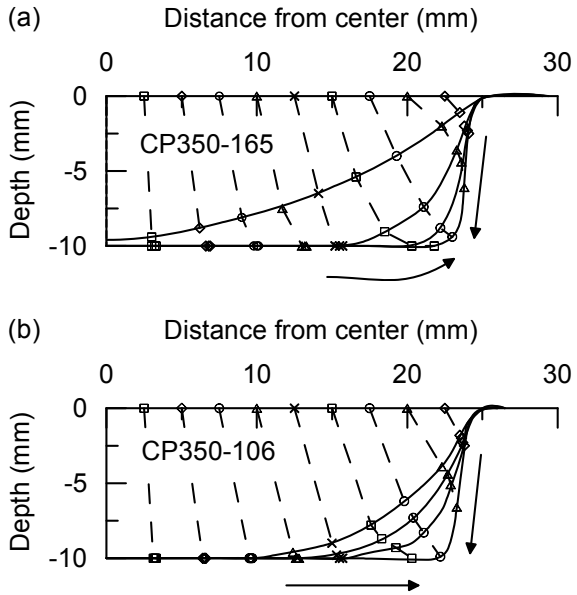

Fig. 9. Deformation contour and metal flow of the sheet during rapid gas blow forming deformed at 350 °C and two different pressures. (a) 2.6 MPa and (b) 3.2 MPa.

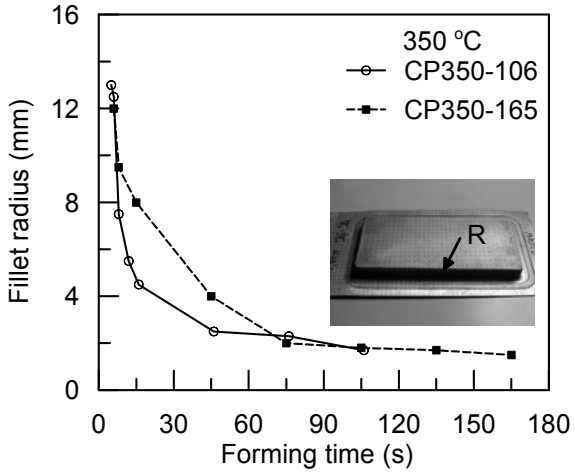

Fig. 10. Variation in fillet radius of the formed pan as a function of forming time deformed at 350 °C and two different pressures.

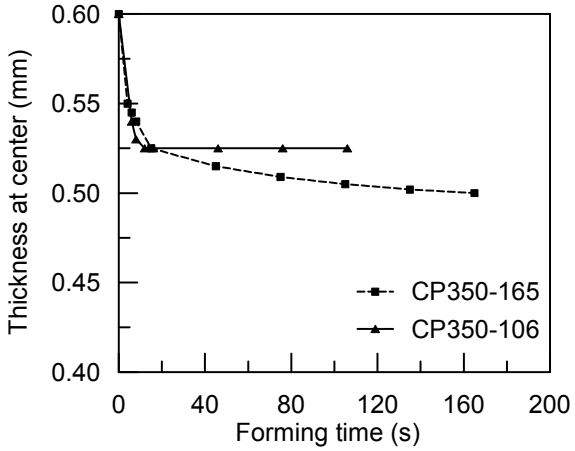

Fig. 11. Variation in thickness at the center point of the formed pan as a function of forming time deformed at 350 °C and two different pressures.

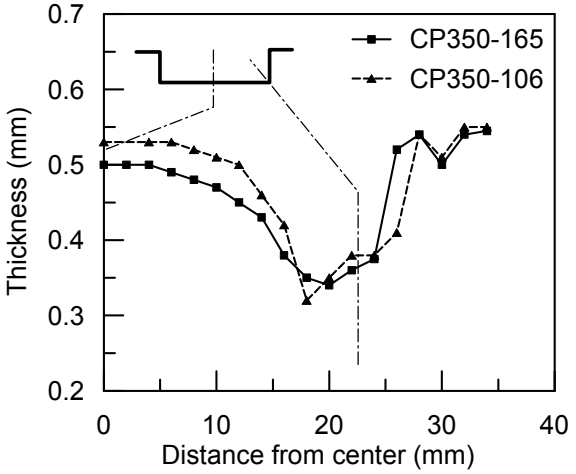

Fig. 12. Thickness distribution along the transverse cross-section of the formed pan deformed at two different pressures and 350 °C.

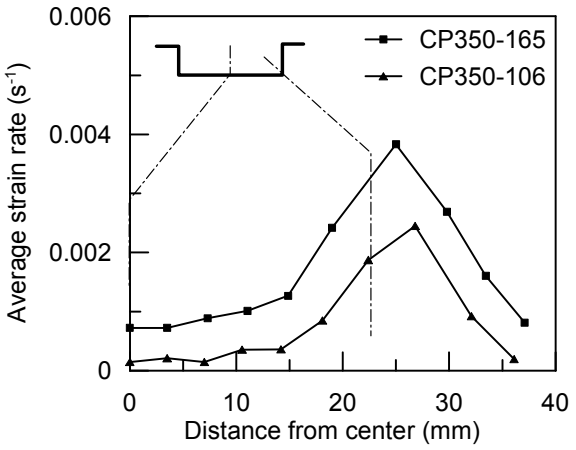

Fig. 13. Average strain rate distribution along the transverse cross-section of the formed pan deformed at two different pressures and 350 °C.

國科會補助計畫衍生研發成果推廣資料表

日期:2011/09/20

國科會補助計畫	計畫名稱: 鎂合金高溫變形機制及快速塑性成形(QPF)研究
	計畫主持人: 吳泓瑜
	計畫編號: 99-2221-E-216-005- 學門領域: 金屬

無研發成果推廣資料

99 年度專題研究計畫研究成果彙整表

計畫主持人：吳泓瑜	計畫編號：99-2221-E-216-005-
計畫名稱：鎂合金高溫變形機制及快速塑性成形(QPF)研究	

成果項目			量化			單位	備註（質化說明：如數個計畫共同成果、成果列為該期刊之封面故事...等）
			實際已達成數（被接受或已發表）	預期總達成數(含實際已達成數)	本計畫實際貢獻百分比		
國內	論文著作	期刊論文	0	0	100%	篇	
		研究報告/技術報告	1	1	100%		
		研討會論文	2	2	100%		
		專書	0	0	100%		
	專利	申請中件數	0	0	100%	件	
		已獲得件數	0	0	100%		
	技術移轉	件數	0	0	100%	件	
		權利金	0	0	100%	千元	
	參與計畫人力（本國籍）	碩士生	0	0	100%	人次	
		博士生	0	0	100%		
		博士後研究員	0	0	100%		
		專任助理	0	0	100%		
國外	論文著作	期刊論文	2	2	100%	篇	
		研究報告/技術報告	0	0	100%		
		研討會論文	0	0	100%		
		專書	0	0	100%	章/本	
	專利	申請中件數	0	0	100%	件	
		已獲得件數	0	0	100%		
	技術移轉	件數	0	0	100%	件	
		權利金	0	0	100%	千元	
	參與計畫人力（外國籍）	碩士生	2	0	100%	人次	
		博士生	1	0	100%		
		博士後研究員	0	0	100%		
		專任助理	0	0	100%		

其他成果 (無法以量化表達之成果如辦理學術活動、獲得獎項、重要國際合作、研究成果國際影響力及其他協助產業技術發展之具體效益事項等，請以文字敘述填列。)	獲邀擔任 2010 Asian Forum on Light Metals (2010 亞洲輕金屬論壇)Invited speaker 及 Co-chair。此項國際學術研討會於 2011 年 10 月 26 至 29 日於中國大陸廣西桂林舉行。

	成果項目	量化	名稱或內容性質簡述
科教處計畫加填項目	測驗工具(含質性與量性)	0	
	課程/模組	0	
	電腦及網路系統或工具	0	
	教材	0	
	舉辦之活動/競賽	0	
	研討會/工作坊	0	
	電子報、網站	0	
	計畫成果推廣之參與（閱聽）人數	0	

國科會補助專題研究計畫成果報告自評表

請就研究內容與原計畫相符程度、達成預期目標情況、研究成果之學術或應用價值（簡要敘述成果所代表之意義、價值、影響或進一步發展之可能性）、是否適合在學術期刊發表或申請專利、主要發現或其他有關價值等，作一綜合評估。

1. 請就研究內容與原計畫相符程度、達成預期目標情況作一綜合評估

■達成目標

□未達成目標（請說明，以 100 字為限）

□實驗失敗

□因故實驗中斷

□其他原因

說明：

2. 研究成果在學術期刊發表或申請專利等情形：

論文：■已發表 □未發表之文稿 □撰寫中 □無

專利：□已獲得 □申請中 ■無

技轉：□已技轉 ■洽談中 □無

其他：(以 100 字為限)

3. 請依學術成就、技術創新、社會影響等方面，評估研究成果之學術或應用價值（簡要敘述成果所代表之意義、價值、影響或進一步發展之可能性）(以 500 字為限)

由拉神實驗的數據顯示，細晶結構鎂合金 AZ31B 快速塑性成形(QPF)是可行的氣壓成形技術。本項技術的建立，對於未來推廣國內鎂合金薄板於 3C 產業的應用具有重要的影響，有助於重建台灣鎂合金成形產業的榮景。鎂合金高溫變形機制的探討及 QPF 快速氣壓成形的關聯性，目前國內外均未見到相關學術論文發表。本研究計畫的成果，已發表國際學術研討會論文，期刊論文也已投寄國外 SCI 等級學術期刊。鎂合金 QPF 成形技術的開發，對國內 3C 產業將會有非常大的實質效益。此項成形技術，也可應用於鋁合金薄殼件及自行車車架的成形製程。